Energy Equip. Sys. / Vol. 9/No. 4/Dec. 2021/ 307-316

ENERGY EQUIPSYS

Energy Equipment and Systems

http://energyequipsys.ut.ac.ir
www.energyequipsys.com

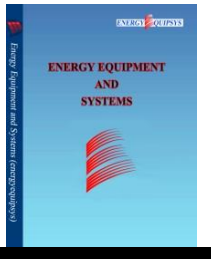

Coordinated control of hybrid AC/DC microgrids including PV and storage systems

Authors

Mitra Nabian Dehaghani [a]
Seyed Abbas Taher [a*]
Zahra Dehghani Arani [a]

[a] Department of Electerical engineering, University of Kashan, Kashan, Iran

Article history:

Received : 30 October 2020
Accepted : 4 July 2021

ABSTRACT

Coordinated control schemes are employed for both bidirectional DC/DC and AC/DC converters in this paper which are considered for connecting AC subgrid to DC one in hybrid AC/DC microgrids. Each subgrid consists of distributed generation units, which are photovoltaic systems working in maximum power point tracking mode, and local loads. Indeed, even though hybrid AC/DC microgrid has multiple merits over conventional microgrid, the interconnection of two different grids has some concerns such as complication, power management, and control. The coordinated control term in bidirectional AC/DC converter is formulated with regard to voltage of common bus and frequency of AC part. The common bus and DC subgrid voltages are utilized in the coordinated control term of bidirectional DC/DC converter. Modeling and simulating a hybrid AC/DC microgrid have been conducted in MATLAB/SIMULINK software. According to simulation results, the surveyed system can sustain its stability under the introduced coordinated control schemes. Hence, the proposed power management system based on coordinated control terms manage the power flow among DC and AC subgrids in addition to storage system.

Keywords: Photovoltaic Systems, Hybrid AC/DC Microgrid, Coordinated Control, Power Management.

1. Introduction

Nowadays, hybrid AC/DC microgrids have become an interesting concept for researchers owing to presence of different DC and AC distributed generations (DGs) including various renewable energy sources and storage systems [1]. These microgrids benefit from advantages of AC and DC microgrids, which are considered as the most possible future systems. They generally include DC subgrid, AC subgrid, bidirectional DC/DC and AC/DC converters (BDDC and BADC), and storage system to connect different subgrids. The AC part has its AC DGs and loads; the DC one also involves DC DGs and loads.

To reach proper power sharing in conventional DC and AC microgrids, several control methods were proposed [2]. Authors in [3] and [4] have investigated fast communication technique-based master-slave control method for DC microgrids. However, this strategy requires communication devices which degrades the

* Corresponding author: Seyed Abbas Taher, Electerical Engineering Department, University of Kashan, Kashan, Iran.
Email: sataher@grad.kashanu.ac.ir

reliability of system. Therefore, the decentralized control strategies employing the $i_{dc} - v_{dc}$ droop method and its derived versions were studied to increase the reliability of DC microgrids [5, 6]. In addition, master-slave strategy was implemented in AC microgrids by Kalke et. al. in [7]. In the proposed scheme, the load demand was compensated completely via slave inverters; voltage and frequency regulation of microgrid were improved under local load variation conditions, as well.

In contrast to conventional DC and AC microgrids, the complexity in controlling hybrid AC/DC microgrids is more challenging. Not only is coordination of two different subgrids associated with well-operating of bidirectional converters, but also the reliability and efficiency of whole microgrid depend on these converters and their control methods. In fact, hybrid AC/DC microgrid operation relies on implementing appropriate power management strategies in order to control the load sharing. Authors of [8] summarized several power management tactics for hybrid AC/DC microgrids. Moreover, an overview and classification were conducted by Unamuno and Barrena in [9] which focused on hierarchical controls in hybrid AC/DC microgrids. Loh et. al. offered a power management strategy to achieve appropriate power interaction that DC voltage and AC frequency were normalized [10]. Considering the balance of power in hybrid AC/DC microgrid, two-stage modified droop control methods, i.e., $\omega - P_{ac}$ and $v_{dc}^2 - P_{dc}$, were suggested by Eghtedarpour and Farjah in [11]. The proposed control method performed power sharing between both subgrids in transition of grid-connected mode to islanded one as well as during the islanded operation which reduce the requested power conversions stages, cost, and efficiency of system. Baharizadeh et. al. proposed a strategy without using frequency variation in controlling structure of hybrid AC/DC microgrid and made it possible to use smaller slope for $f - P_{ac}$ droop characteristic [12]. Thus, smaller frequency variation and better power quality were achieved at AC side. A cascade P_{dc}/V_{dc} control with a wide constant band for power has been adopted in [13] that efficient usage of photovoltaic (PV) generation gained in a hybrid AC/DC microgrid. Considering battery converter, a new P_{dc}/V_{dc} droop control strategy with narrow band was introduced to prevent from exceeding of voltage limit. However, the load power quality limited the width of mentioned band. A novel decentralized control technique for hybrid AC/DC microgrid was presented in [14] by Baharizadeh et al. which is based on recent characteristics of droop method for sources and inverters, and adjusting the voltage magnitude of a common bus in each subgrid. Gundabathini and Pindoriya used a control system along with optimal switching approach which can enhance power flow control capability of bidirectional converter and various operation states in hybrid AC/DC microgrid [15]. In [16], a new BADC topology was presented and an independent power control method was designed which caused two subgrids to backup each other. Supposing distributed storages (DSs), authors in [17] recommended a distributed strategy for regulating and managing power of a three-port hybrid AC/DC microgrid, involving DS, DC, and AC subgrids. A common hierarchical control manner similar to the control system of only DC or AC microgrid was made for the hybrid AC/DC microgrid in [18]. Moreover, several intelligent control systems were utilized for supervising power of such hybrid microgrid. Authors of [19] offered a fuzzy control strategy for hybrid AC/DC microgrid to handle the power of battery energy storage systems. In these available schemes for managing power in hybrid AC/DC microgrids, a coordinated control term is only utilized commonly in the control structure of BADC. However, it has been rarely considered coordinated control term in the control structure of BDDC. On the other hand, maintaining a stable operation for both DC and AC subgrids, appropriate power sharing, causing subgrids to stand up for each other, and coordinately sharing power fluctuations of system are difficult in hybrid AC/DC microgrid. Hence, a simple strategy for coordinated control of hybrid AC/DC microgrids that can address aforementioned issues is necessary.

In this paper, a hybrid AC/DC microgrid including PV as well as battery energy storage systems is considered to reduce processes of power conversions. Hence, the interconnection of diverse sources as well as loads to power system can be simplified. Maximum power point

tracking (MPPT) mode is considered for PV systems. According to the common bus voltage, voltage of DC part, and frequency of AC part, an effective coordinated power control technique is designed and applied to control structures of both BADC and BDDC to achieve mentioned purposes. In fact, the principal contributions of this paper are:

- The correction term based on common bus voltage and AC frequency is unified with droop control method in control structure of BADC.
- The common bus and DC subgrid voltages-based coordinated control term is proposed to use in combination with droop control method for BDDC.
- The battery energy storage system located in the storage system can sustain the stability of common bus voltage.

Figure 1 displays the flowchart for main contributions and methods presented for managing power in hybrid AC/DC microgrid.

The rest of this research is presented in next sections. The structure of hybrid AC/DC microgrid under study, PV model, proposed coordinated method, droop control strategy for BADC and BDDC, and storage system control are given in Section 2. Section 3 exhibits the results of simulation. Eventually, Section 4 concludes this research.

2. System configuration, modeling, and control

2.1. Hybrid AC/DC microgrid topology

Figure 2 demonstrates the investigated configuration of the hybrid AC/DC microgrid. The AC subgrid has AC DG and load, that its DG is a PV system working in MPPT mode. The DC subgrid also has its DC DG and load; its DG is a PV system working in MPPT mode as well. These subgrids are connected through bidirectional power converters.

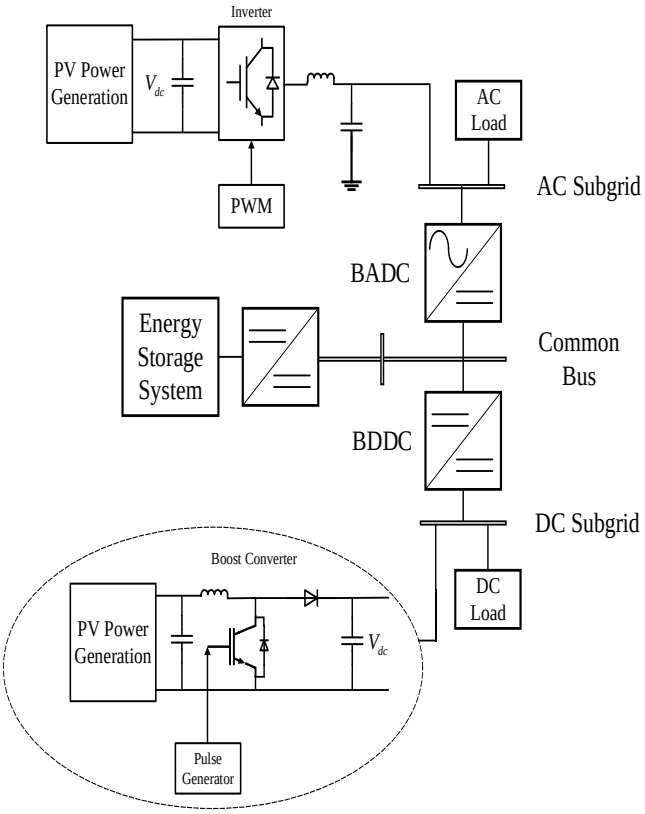

Fig. 2. The investigated hybrid AC/DC microgrid

2.2. Modeling of PV system

The equivalent circuit of a PV module connected to a load is illustrated in Fig.3. The PV system output current can be modeled by next three equations [20]. Parameters of Sun Power SPR-305E-WHT-D PV system used in this paper are presented in Table 1.

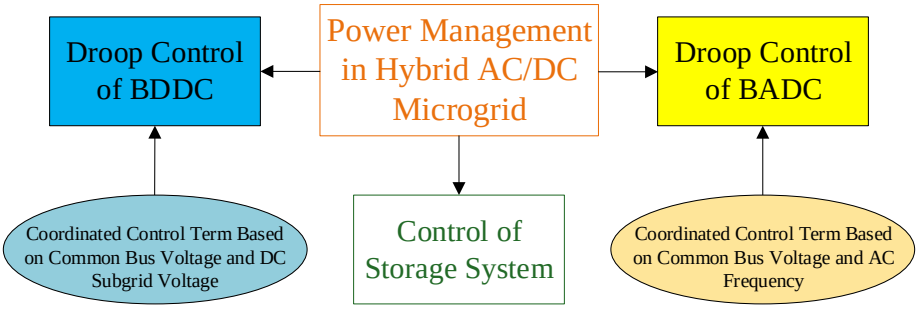

Fig. 1. Flowchart of main contributions and methods

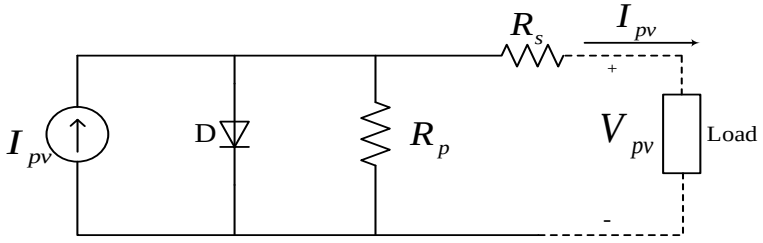

Fig. 3. Equivalent model of a PV module

Table 1. Parammeters of PV system

Symbol	Description	Value
V_{oc}	Rated open circuit voltage	64.2 V
I_{ph}	Photocurrent	6.009 A
I_{sat}	Module reverse saturation current	6.3×10^{-12} A
q	Electron charge	1.6×10^{-19}
A	Ideality factor	150
K	Boltzman constant	1.38×10^{-23}
R_s	Series resistance of PV cell	0.37152 Ω
R_p	Parallel resistance of PV cell	269.5934 Ω
I_{sc}	Short-circuit current	5.96 A
V_{mp}	Voltage at maximum power point	54.7 V
I_{mp}	Current at maximum power point	5.58 A
T_r	Reference temperature	1.7×10^{-3}
I_{rr}	Reverse saturation current at T_r	
E_{gap}	Energy of the band gap for silicon	1.1eV
S	Solar radiation level	1000 W/m^2
T	Surface temperature of PV	50 ^{0}C

$$I_{pv} = n_p I_{ph} - n_p I_{sat} \times [\exp((\frac{q}{AkT})(\frac{V_{pv}}{n_s} + I_{pv} R_s))^{-1}] \quad (1)$$

$$I_{ph} = (I_{sc} + k_i (T - T_r)).\frac{S}{1000} \quad (2)$$

$$I_{sat} = I_{rr}\left(\frac{T}{T_r}\right)^3 \exp((\frac{qE_{gap}}{kA}) \times (\frac{1}{T_r} - \frac{1}{T})) \quad (3)$$

Both subgrids comprise PV-based DGs which work in MPPT mode. The implemented MPPT algorithm is conducted by using the "incremental conductance and integral regulator" technique. In fact, MPPT controller optimizes the switching duty cycle to generate the required voltage. Plenty of control methods for AC or DC grids have been probed in numerous researches [21, 22]. The PV plant is pinned to DC microgrid via a DC/DC boost converter [23]. This DC/DC boost converter increases PV voltage to desired value.

2.3. Coordinated power control among subgrids

A strategy for managing the power of PV-based hybrid AC/DC microgrid is presented in this subsection. In this microgrid, the interaction among DC and AC parts is more complicated than conventional only DC or AC microgrids. On the condition that the power is in surplus (or in shortage) in either DC or AC parts, values of DC voltage or AC frequency will be higher (or lower). Hence, in light of corresponding frequency and voltage changes, the coordinated power control scheme is presented. The utilized control law for this microgrid is as follows which is shown in Fig.4:

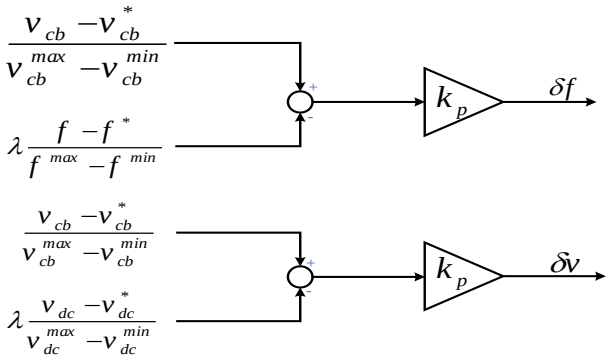

Fig. 4. Coordinated power control strategy for bidirectional converters

$$\delta f = \left(k_p\right)\left(\frac{v_{cb}-v_{cb}^{*}}{v_{cb}^{max}-v_{cb}^{min}}-\lambda\frac{f-f^{*}}{f^{max}-f^{min}}\right)$$
$$\delta v = \left(k_p\right)\left(\frac{v_{cb}-v_{cb}^{*}}{v_{cb}^{max}-v_{cb}^{min}}-\lambda\frac{v_{dc}-v_{dc}^{*}}{v_{dc}^{max}-v_{dc}^{min}}\right) \quad (4)$$

where δf and δv are yields of coordinated control which are transferred to bidirectioanl converters. k_p is the coefficient of proportional (P) controllers. Also, v_{cb}^{*}, v_{dc}^{*}, and f^{*} are rated values of common bus voltage, DC subgrid voltage, and AC frequency, respectively. In addition, v_{cb}, v_{dc}, and f are actual common bus voltage, DC subgrid voltage, and AC frequency, respectively. It should be mentioned that maximum and minimum values of these variables are illustrated by the superscripts max and min, respectively. For proper performance of the microgrid, the subgrids are not allowed to change their electrical parameters while the proportion of critical loads increases [24]. In this research, to over come this problem, the correction coefficient, λ, is used which can be adjusted as:

$$\lambda = \left(\frac{P_i^{sum}}{P^{sum}}\right)^{-1}\cdot\frac{P^{cri}}{P^{sum}} \quad (5)$$

Where P_i^{sum} is total capacity, P^{cri} is critical load capacity in subgrids, and total capacity of the entire microgrid is considered as P^{sum}. It is notable that larger correction coefficient should be designed for smaller capacity and larger ratio of critical loads. As BADC and BDDC contain the local feedback variables, the presented coordinated power control is a decentralized method, which improves the reliability of whole system.

2.4. Droop control for BADC and BDDC

In present research, the conventional droop control is employed for BADC and BDDC. Figure 5 shows the structure and control method of BADC, which its AC part connects to AC subgrid via a LC filter and DC part connects to common bus. The entire control structure involves two loops, which interior one controls the output voltage and exterior loop comprises reactive power-voltage and active power-frequency droop equations for generating reference values for interior loop. The droop equations are stated as follows [24].

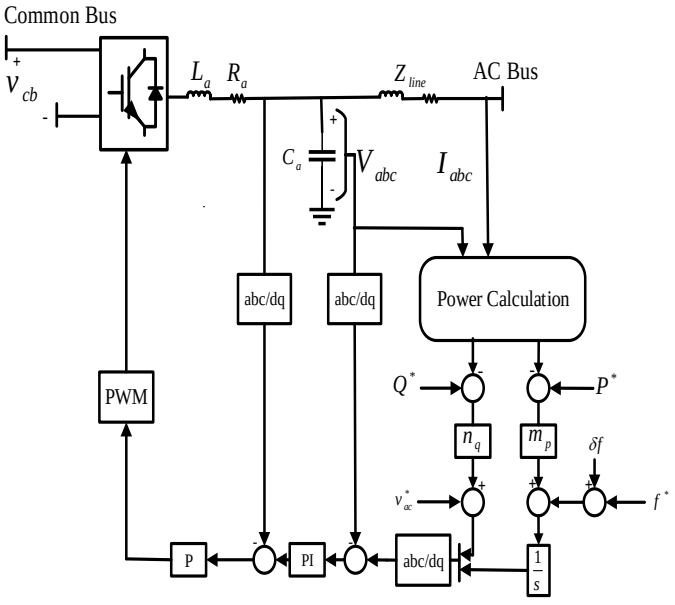

Fig. 5. Structure and control method of BADC

$$f^{ref} = \left(f^* + \delta f \right) + m\left(P^* - P \right)$$
$$v^{ref} = v^* + n\left(Q^* - Q \right) \quad (6)$$

where v^{ref} and f^{ref} are reference values of voltage and frequency for interior loop, respectively. v^* and f^* are rated voltage and frequency, m and n are droop coefficients, Q^* and P^* are rated reactive and active powers, and Q and P are actual reactive and active powers, respectively. δf is obtained by coordinated control scheme for BADC.

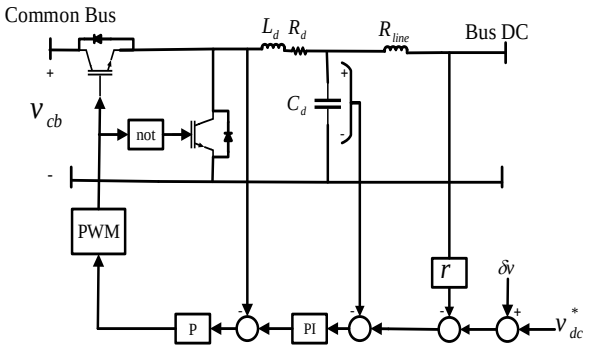

Fig. 6. Structure and control method of BDDC

Configuration and corresponding control of BDDC are shown in Fig.6. The entire control strategy includes two interior and exterior loops. The exterior one uses $i_{dc} - v_{dc}$ droop control method for generating reference value for interior loop, which is expressed as [5]

$$v_{dc}^{ref} = \left(v_{dc}^* + \delta v \right) - r \cdot i_{dc} \quad (7)$$

where v_{dc}^{ref} is the reference value of DC output voltage of interior loop. In addition, r is droop coefficient and i_{dc} is actual value of DC output current. The coordinated power control generates δv of BDDC as well.

2.5. Control of storage system

Storage system is utilized for sustaining the voltage of common bus and balancing power of whole grid. Figure 7 depicts the structure and control method of this system. As depicted in this figure, the bidirectional DC/DC converter connects the battery to the common bus. In the control system, the static error of common bus voltage is firstly eliminated with a proportional-integral (PI) controller. Then, in order to intensify damping and improve the stability, a P controller is employed. It should be noted that C_s, R_s, and L_s are capacitance, resistance, and inductance of the filter, respectively. Also, battery voltage is written as V_s that can be almost considered as a constant DC voltage source.

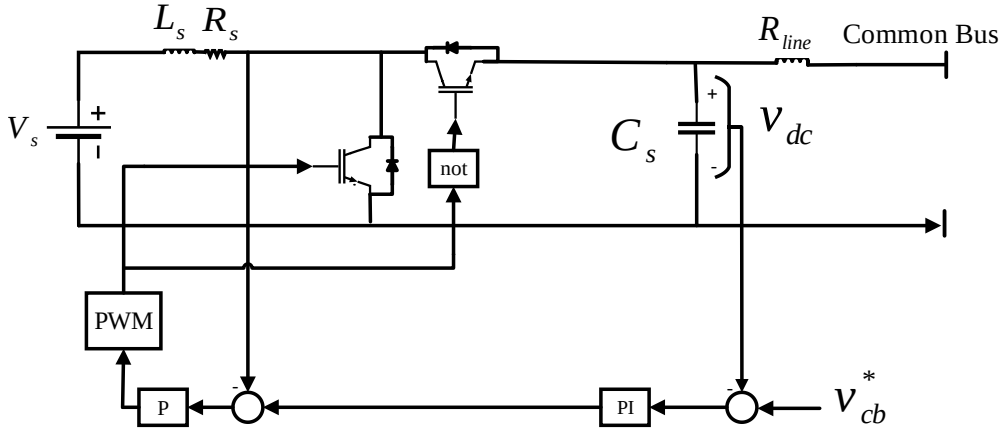

Fig. 7. Structure and control method of storage system

3. Results and discussions

In this section, simulation and its results are shown for verifying the proficiency of coordinated power control in hybrid AC/DC microgrid illustrated in Fig.2.

The rated frequency of AC subgrid is 50 Hz with acceptable change range of ±0.5 Hz. The AC subgrid voltage magnitude is equal to 311 V. The powers of rated and critical loads are 60 kW+j16 kVAr and 40 kW, respectively. The output power of AC DG, which works in MPPT mode, is 40 kW.

The rated value of DC subgrid voltage is 500 V with acceptable change range of ±25 V. The powers of rated and critical loads are 80 kW and 20 kW, respectively. The output power of DC DG operating in MPPT mode, is 60 kW.

The storage system sustains the voltage of common bus which its nominal value is 1000 V with acceptable change range of ±50 V. The battery nominal voltage is 600 V. Tables 2, 3, and 4 show the parameters of storage system, BDDC, and BADC, respectively.

Table 2. Parameters of storage system

Electrical Parameters	**VALUE**
Battery voltage	V_s =600 V
Rated common bus voltage	v_{cb}^* =1000 V
Inductive filter	L_s =1.5 mH R_s =1 mΩ
Capacitive filter	C_s =8 mF
Line resistance	R_{line} =7 mΩ
Controller Parameters	**VALUE**
Voltage controller (PI)	k_p =0.7 k_i =70
Current controller (P)	k_p =8

Table 3. Parameters of BDDC

Electrical Parameters	**VALUE**
Rated DC bus voltage	v_{dc}^* =500 V
LC filter	L_d =2 mH R_d =1 mΩ
Capacitive filter	C_d =8 mF
Line resistance	R_{line} =10 mΩ
Controller Parameters	**VALUE**
Coordinated power controller	λ =1.41 k_p =1.5
Droop controller	r =0.7
Voltage controller (PI)	k_p =0.6 k_i =50
Current controller (P)	k_p =3

Table 4. Parameters of BADC

Electrical Parameters	**VALUE**
Rated AC bus voltage	v_{ac}^* =311 V
Rated AC frequency	f =50 Hz
LC filter	L_a =2.5 mH R_a =1 mΩ
Capacitive filter	C_a =2 mF
Line impedance	Z_{line} =0.8 mH+1 mΩ
Controller Parameters	**VALUE**

Coordinated power controller	λ =4 k_p = 0.03
Droop controller	P^* =20 kW, Q^* =10 kVAr m_p =5 Hz/MW n_q =0.1 V/kVAr
Voltage controller (PI)	k_p =0.8 k_i =100
Current controller (P)	k_p =4

The hybrid AC/DC microgrid under study operates under rated load powers in AC and DC subgrids up to t=5 s. The AC critical load is connected at t=5 s. Finally, at t=10 s, DC critical load is added. Figures 8-10 demonstrate the dynamic responses of hybrid AC/DC microgrid with proposed coordinated power control strategy under these case studies.

The AC frequency, common bus voltage, and DC subgrid voltage are shown in Fig.8. It is observed that as AC subgrid load power increases at t=5 s, AC subgrid frequency decreases. Also, the DC subgrid voltage decreases when the DC critical load is connected. It should be noted that the storage system regulates the common bus voltage under load power variation conditions accurately.

Figure 9 indicates that the fluctuations of AC frequency, common bus voltage, and DC subgrid voltage are in their acceptable ranges, where $\Delta f = f^* - f$, $\Delta v_{cb} = v_{cb}^* - v_{cb}$, and $\Delta v_{dc} = v_{dc}^* - v_{dc}$. Also, f^*, v_{cb}^*, and v_{dc}^* are equal to 50 Hz, 1000 V, and 500 V, respectively.

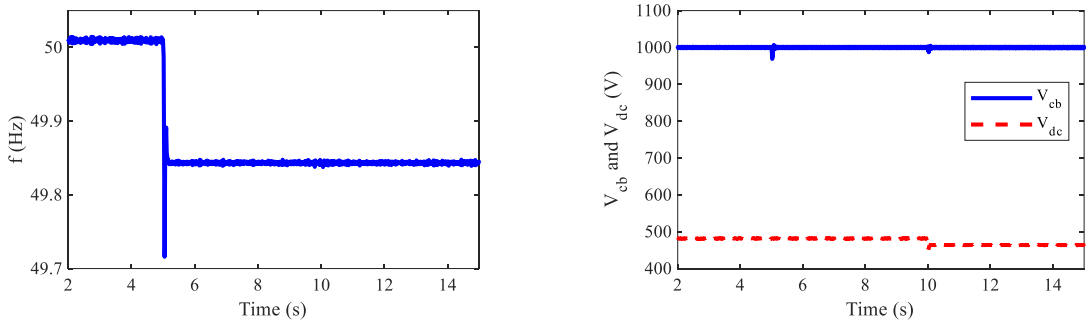

(a) (b)

Fig. 8. (a) AC frequency, (b) Common bus and DC subgrid voltages

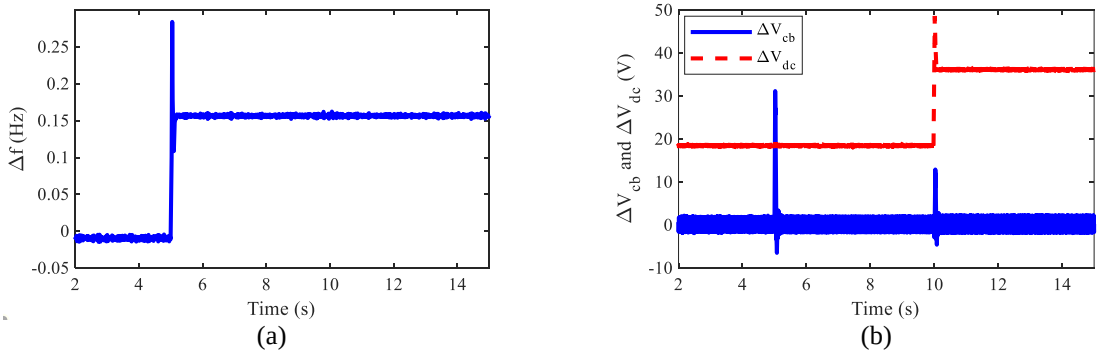

(a) (b)

Fig. 9. (a) Variation of AC frequency, (b) Variation of common bus and DC subgrid voltages

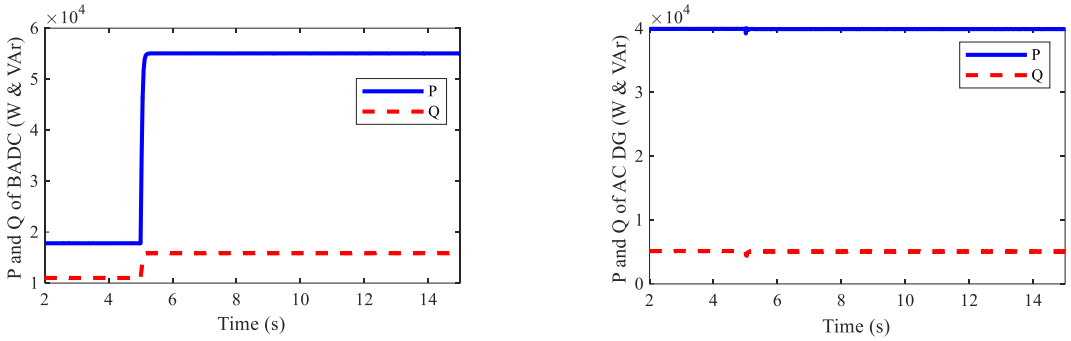

(a) (b)

Fig. 10. Active and reactive powers: (a) from BADC, (b) from AC DG

As Fig.10 illustrates, the AC DG works in MPPT mode with constant output active and reactive powers under load power variations. Also, the output active and reactive powers of BADC increase by adding the AC critical load at t=5 s. From simulation results, it is obvious that the introduced coordinated strategy for power management can operate properly, which shows its high reliability.

4. Conclusion

This paper recommended an efficient coordinated control technique for a hybrid AC/DC microgrid which its correction terms were applied to control systems of BADC as well as BDDC. Both common bus voltage and AC frequency were used in the coordinated control term of BADC. The coordinated control term of BDDC was implemented according to the voltages of common bus and DC subgrid. This control strategy provided

- proper and stable operation of storage system as well as AC and DC subgrids,
- proper power interplay between different subgrids,
- and ensuring that both subgrids support each other under power fluctuation conditions.

The effectiveness of proposed method was evaluated by the simulations, which satisfied power management. For future researches, the effect of primary control systems of BADC and BDDC, which was droop control scheme in this research, on the presented coordinated control strategy can be investigated.

References

[1] Liu, X., Liu, X., Wang, P., and Loh, P. C., A Hybrid AC/DC Microgrid and its Coordination Control. IEEE Transactions on Smart Grid, (2011), 2(2):278-286.

[2] Guerrero, J. M., Vasquez, J. C., Matas, J., De Vicuña, L. G., and Castilla, M., Hierarchical Control of Droop-Controlled AC and DC Microgrids, A General Approach Toward Standardization, IEEE Transactions on Industrial Electronics, (2011), 58(1):158-172.

[3] Francesco, D., Enrico, P., Stefano, S., High Voltage DC/DC Converter with Master/Slave Buck Output Stages, European Patent Application, (2015), EP 2 894 776 A1.

[4] Federico, I., Jose, E., Luis, F., Master -Slave DC Droop Control for Paralleling Auxiliary DC/DC Converters in Electric Bus Applications, IET Power Electronics, (2017), 10(10):1156-1164.

[5] Huang, P. H., Liu, P. C., Xiao, W., and El Moursi, M. S., A Novel Droop-Based Average Voltage Sharing Control Strategy for DC Microgrids, IEEE Transactions on Smart Grid, (2015), 6(3):1096-1106.

[6] Xia, Y., Peng, Y., Hu, H., Wang, Y., and Wei, W., Advanced Unified Decentralised Control Method with Voltage Restoration for DC Microgrids, IET Renewable Power Generation, (2016), 10(6):861-871.

[7] Kalke, D., Suryawanshi, H. M., Talapur, G. G., Deshmukh, R., Nachankar, P., Modified Droop and Master-Slave Control for Load Sharing in Multiple Standalone AC

Microgrids, 5th Annual Conference of the IEEE Industrial Electronics Society, (2019).
[8] Nejabatkhah, F., and Li Y. W., Overview of Power Management Strategies of Hybrid AC/DC Microgrid, IEEE Transactions on Power Electronics, (2015), 30(12):7072-7089.
[9] Unamuno, E., Barrena, J. A., Hybrid AC/DC Microgrids—Part II: Review and Classification of Control Strategies, Renewable and Sustainable Energy Reviews, (2015) 52:1123-1134.
[10] Loh, P. C., Li, D., Chai, Y. K., and Blaabjerg, F., Autonomous Operation of Hybrid Microgrid with AC and DC Subgrids, IEEE Transactions on Power Electronics, (2013), 28(5):2214-2223.
[11] Eghtedarpour, N., and Farjah E., Power Control and Management in a Hybrid AC/DC Microgrid, IEEE Transactions on Smart Grid, (2014), 5(3):1494-1505.
[12] Baharizadeh, M., Karshenas, H. R., Guerrero, J. M., Control Strategy of Interlinking Converters as the Key Segment of Hybrid AC/DC Microgrids, IET Generation Transmission & Distribution, (2016), 10(7):1671-1681.
[13] Han, H., Shen, L., Yang, J., Su, M., The Coordinated Control Strategy of Hybrid Microgrid Based on the Maximum Utilization of PV Generation, Chinese Automation Congress (CAC), (2015), 1416-142.
[14] Baharizadeh, M., Karshenas, H. R., Guerrero, J. M., An Improved Power Control Strategy for Hybrid AC/DC Microgrids, International Journal of Electrical Power & Energy Systems, (2018), 95:364.
[15] Gundabathini, R., Pindoriya, N. M., Improved Control Strategy for Bidirectional Single Phase AC/DC Converter in Hybrid AC/DC Microgrid, Electric Power Components and Systems, (2017),45(20):2293-2303.
[16] Loh, P. C., Li, D., Chai, Y. K., and Blaabjerg, F., Autonomous Control of Interlinking Converter with Energy Storage in Hybrid AC/DC Microgrid, IEEE Transactions on Industry Applications, (2013), 49(3):1374-1382.
[17] Wang, P., Jin, C., Zhu, D., Tang, Y., Loh, P. C., and Choo, F. H., Distributed Control for Autonomous Operation of a Three-Port AC/DC/DS Hybrid Microgrid, IEEE Transactions on Industrial Electronics, (2015), 62(2):1279-1290.
[18] Majumder, R., Chaudhuri, B., Ghosh, A., Majumder, R., and Ledwich, G. F., Improvement of Stability and Load Sharing in an Autonomous Microgrid Using Supplementary Droop Control Loop, IEEE Transactions on Power Systems, (2010), 25(2):796-808.
[19] Xia, Y., Peng, Y., Wei W., Triple Droop Control Method for AC Microgrids, IET Power Electronics, (2017), 10(13):1705-1713.
[20] Mahmood, F., Va nfretti, L., Hooshyar H., Modeling of a Detailed Photovoltaic Generation System for EMT-Type Simulation, IEEE International Energy Conference (ENERGYCON), (2014).
[21] Zhong, Q. C., Robust Droop Controller for Accurate Proportional Load Sharing Among Inverters Operated in Parallel, IEEE Transactions on Industrial Electronics, (2013), 60(4):1281-1290.
[22] Bidram, A., Davoudi, A., Lewis, F. L., and Guerrero, J. M., Distributed Cooperative Secondary Control of Microgrids Using Feedback Linearization, IEEE Transactions on Power Systems, (2013), 28(3):3462-3470.
[23] Hong, Z., Xu, Y., He, J., Ni, P., Yao, Y., Average-Value Modeling of Photovoltaic Generation Systems, IEEE 8th Annual International Conference on CYBER Technology in Automation, Control, and Intelligent Systems (CYBER), (2018).
[24] Xia, Y., Wei, W., Yu, M., Wang, X., and Peng, Y., Power Management for a Hybrid AC/DC Microgrid with Multiple Subgrids, IEEE Transactions on Power Electronics, (2017), 33(4):3520-3533.